



Universiteit  
Leiden  
The Netherlands

## Water on well-defined platinum surfaces : an ultra high vacuum and electrochemical study

Niet, M.J.T.C. van der

### Citation

Niet, M. J. T. C. van der. (2010, October 14). *Water on well-defined platinum surfaces : an ultra high vacuum and electrochemical study*. Retrieved from <https://hdl.handle.net/1887/16035>

Version: Corrected Publisher's Version

License: [Licence agreement concerning inclusion of doctoral thesis in the Institutional Repository of the University of Leiden](#)

Downloaded from: <https://hdl.handle.net/1887/16035>

**Note:** To cite this publication please use the final published version (if applicable).

*Diviser chacune des difficultés que j'examinerais, en autant de parcelles qu'il se pourroit, et qu'il seroit requis pour les mieux résoudre.*

René Descartes, Discours de la méthode, Seconde partie (1637)

# 1

## Introduction

### 1.1 Heterogeneous catalysis

---

Catalysis is an extremely important phenomenon in our modern industrial world. A catalyst is defined as a material which can enhance the rate of a reaction. It is intimately involved in the reaction sequence, but is regenerated at the end of it. The production of approximately 90% of all chemicals and materials requires a catalyst. Nature is also full of catalysts in the form of enzymes, which are vital to all chemical reactions taking place in organisms. Humans have been using catalysts for millennia, ever since they learned how to use natural yeasts to ferment fruit to yield alcoholic drinks. Early in the 19th century a more systematic study of the phenomenon began.

Industrial catalysis can be divided into heterogeneous and homogeneous catalysis. In heterogeneous catalysis the reactants and the catalyst are in a different phase. The catalyst is often solid, whereas the reactants are gaseous or liquid. In homogeneous catalysis the reactants and the catalyst are in the same phase. Heterogeneous catalysis is most often used in modern industry, since it is much easier to separate the catalyst from the reactants and products. All research described in this thesis concerns heterogeneous catalysis.

In heterogeneous catalysis the surface of a particle acts as the catalyst. The surface is an abrupt termination of the bulk structure. Surface atoms can only form bonds with neighboring atoms in the surface plane and in the bulk. Free bonds are left on the surface, which can interact with incoming molecules. A first step in heterogeneous catalysis is often the adsorption of a molecule to the surface. This can happen through either dissociative chemisorption (the molecular bond of the incoming molecule is broken and the separate fragments form new bonds with the surface instead), molecular chemisorption (the molecular bonds of the molecule stay intact and additional bonds with the surface are formed), or physisorption. Different species adsorbed at the surface can interact with one another, forming new compounds, which consecutively desorb off the surface.<sup>1</sup>

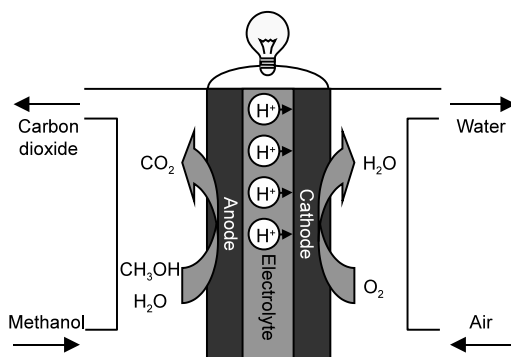
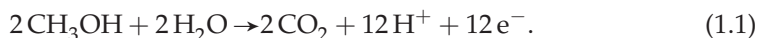


Figure 1.1 Schematic workings of a methanol fuel cell.<sup>2</sup>

## 1.2 Fuel cells

Ever since the industrial revolution, mankind relies on fossil fuels (coal, oil, and natural gas) to provide us with energy. Over the last decades it has become clear that stocks are running out. Another problem is that when fossil fuels are burned,  $\text{CO}_2$  is formed: a greenhouse gas.<sup>3</sup> Both science and industry are searching for new energy sources. An attractive alternative to the use of fossil fuels are fuel cells, which can use either hydrogen, methanol, or ethanol as an energy source. Figure 1.1 shows schematically how a methanol fuel cell works; methanol and water react at the anode via



The formed protons are transported through a membrane to the cathode, where oxygen from air reacts via



This makes carbon dioxide and water the only reaction products. The flow of electrons, traveling from anode to cathode, is electricity. Since both methanol and ethanol can be produced from renewable sources, where  $\text{CO}_2$  is consumed, the  $\text{CO}_2$  formed in a fuel cell does not net contribute to the greenhouse effect. Hydrogen fuel cells only have water as a reaction product.

For both cathode and anode, platinum is often the catalyst material of choice. However, platinum is expensive, relatively scarce and becomes poisoned in the long run. Therefore, it is important to search for cheaper and better catalysts. In order to do this it is vital to understand why platinum is such a good catalyst. When it comes to understanding platinum catalysts, one of the fundamental questions is the state of adsorbed water at the platinum surface at various potentials. In direct alcohol fuel cells, water will have to dissociate in order for its oxygen atom to

react with the carbon atoms, forming  $\text{CO}_2$ . The question is whether it dissociates into OH fragments or oxygen atoms before it reacts. In this thesis we will model the platinum fuel cell electrode under both electrochemical and ultra high vacuum conditions to answer this question.

## 1.3 Ultra high vacuum modeling

---

One way to obtain more information on the state of the water on the surface would be to use infrared (IR) spectroscopy. However, detecting OH in a aqueous environment is very difficult, since the peaks overlap with peaks originating from water. The problem can be simplified by studying the system in ultra high vacuum (UHV). The amount of molecules present in a UHV system is small enough to keep a platinum sample clean for 2–3 hours to do experiments. The amount of adsorbate can be easily controlled by leaking in different amounts of gas. Numerous techniques can be used in order to study the interactions between surface and adsorbates, as well as between adsorbates.<sup>4</sup> In this thesis we mainly use temperature programmed desorption (TPD), low energy electron diffraction (LEED), and reflection absorption infrared spectroscopy (RAIRS). More details about these techniques will be given in chapter 2.1.

A major draw-back of UHV modeling, however, is that it does not represent realistic catalytic conditions. This is usually referred to as the pressure gap, since the pressures in UHV are much lower than in a reactor ( $< 10^{-7}$  mbar vs.  $\geq 1$  atm). This often results in the use of lower temperatures as well, in order for the adsorbates to remain at the surface. When comparing to the electrochemical environment in particular, it is also difficult to model the electrochemical double layer, where both negative and positive ions are present, along with a potential gradient. The inclusion of all these factors is not necessarily trivial to the reaction of adsorbates with both the surface and with one another. Nonetheless, UHV experiments can provide invaluable information about the interactions between reactants, because of the relative simplicity of the data.

## 1.4 Model catalysts

---

Figure 1.2a shows a schematic representation of a catalyst nanoparticle.<sup>5</sup> It is complex: many different sites are available for a reaction, all with very different geometries. This makes it difficult to study real catalyst particles in order to understand fundamental reaction steps; there are simply too many options. Instead of nanoparticles we use single crystals as model catalysts, since here we know exactly what the surface geometry is. The simplest surface is the Pt(111) surface (figure 1.2b), which has a hexagonal structure. Much research on this surface has been done, giving us

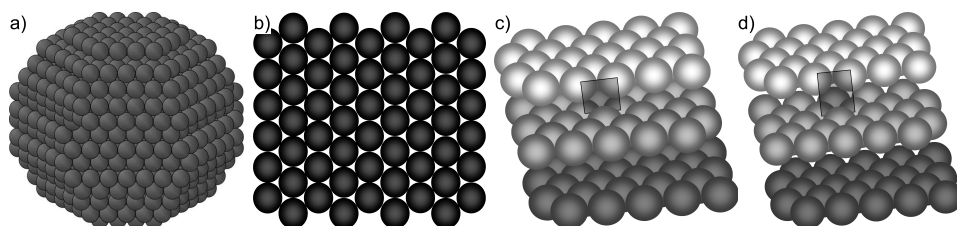


**Figure 1.2** a) A catalyst nanoparticle,<sup>5</sup> b) the Pt(111) surface, c) the stepped Pt(533) surface, and d) the stepped Pt(553) surface.

a reasonable understanding of *e.g.*  $\text{H}_2\text{O}$ ,  $\text{O}_2$ , and  $\text{H}_2$  adsorption on this surface.<sup>6–12</sup> However, the infinite (111) structure of the Pt(111) surface is very remote from the structure shown in figure 1.2a. This is often referred to as the material gap. On catalyst particles the reactivity is thought to be mainly due to the presence of step, edge, and defect sites.<sup>13</sup> One step closer to real catalyst particles are stepped surfaces (figure 1.2c and d). Here, defects are introduced in a controlled manner. This gives a more realistic model of catalyst particles, while keeping the interpretation of the data still relatively simple. Figure 1.2c shows the Pt(533) surface, which consists of four atom wide terraces with a (111) geometry with a monoatomic step of (100) geometry (indicated by the black marker). The Pt(553) surface has the same terrace width, but with monoatomic steps of the (110) geometry (figure 1.2d), which gives the surface a more slanting nature than the Pt(533) surface. The study of many single crystals with (slightly) different geometries should eventually lead to a better understanding of real catalysts.

## 1.5 Scope of this thesis

---

In this thesis we will investigate the dissociation state of water on platinum electrodes, as stated in section 1.2. First we will have a separate look at the interaction of water's building blocks with single crystal platinum surfaces under UHV conditions: chapter 3 will describe the influence of the step geometry (100) or (110) on the desorption characteristics of  $\text{O}_2$ ,  $\text{D}_2$ , and  $\text{H}_2\text{O}$ .

Under UHV conditions OH groups can be formed on Pt(111) by pre-covering the surface with O adatoms, causing water to dissociate. The formed OH-groups are incorporated in a hydrogen bonded network of OH/ $\text{H}_2\text{O}$  at the surface.<sup>14,15</sup> A similar tactic could lead to the formation of OH at step sites at stepped platinum surfaces. This hypothesis will be tested in chapters 4–6 for the two different step types shown in figure 1.2c and d.

Another interesting co-adsorbant from an electrochemical point of view is hydrogen. Both in the hydrogen fuel cell as well as in the often used reversible hy-

drogen electrode, water and hydrogen are simultaneously present at the catalyst. Chapters 7–9 will discuss the co-adsorption of these species at stepped platinum surfaces with different step geometries.

Chapters 10 and 11 will discuss experiments under electrochemical conditions. Chapter 10 will discuss the impedance spectroscopy of water dissociation in both alkaline and acidic electrolyte for Pt(111) and platinum surfaces with (110) step sites. Chapter 11 will give a model for the oxidation state of water at step sites at various potentials, which is to a large extent based on the results obtained in the previous chapters.

## 1.6 Literature overview

---

Before we describe the research for this thesis, we will give a brief overview of what is known about the systems we study from literature.

### 1.6.1 Water on platinum

Three extensive reviews have appeared that summarize the large body of knowledge on water-surface interactions that has been obtained using a variety of surfaces, co-adsorbates, and employed techniques.<sup>6–8</sup> The general consensus is that on Pt(111) water adsorbs molecularly at all coverages and temperatures ( $< 180$  K). Even prolonged exposure to X-rays does not cause dissociation in the water layer.<sup>16</sup> Classically, water adsorbed on metal surfaces is thought to form an ice-like bilayer of hexagonal rings.<sup>6–8</sup> Low energy electron diffraction (LEED)<sup>17</sup> and helium diffraction<sup>18</sup> images show a  $(\sqrt{37} \times \sqrt{37})R25.3^\circ$  structure for H<sub>2</sub>O islands formed at submonolayer coverage on Pt(111), which is compressed into a  $(\sqrt{39} \times \sqrt{39})R16.1^\circ$  structure for the full bilayer. A combined scanning tunneling microscopy (STM) and density functional theory (DFT) study finds these “ $\sqrt{37}$ ” and “ $\sqrt{39}$ ” phases to also contain pentagon and heptagon structures.<sup>19</sup> An extensive high resolution electron energy loss spectroscopy (HREELS) study by Jacobi *et al.* shows distinct differences in the vibrational spectra for water monomer, bilayer, and multilayer structures.<sup>20</sup>

Water dosed on Pt(111) at temperatures well below 135 K leads to the formation of amorphous solid water (ASW).<sup>21</sup> Temperature programmed desorption (TPD) studies of ASW show two peaks. One peak at 171 K is associated with monolayer desorption. This peak exhibits the characteristics of zero-order desorption kinetics<sup>22</sup> and has been attributed to the co-existence of a condensed phase and a 2-dimensional water-gas at submonolayer coverages.<sup>21</sup> A second peak, associated with desorption from multilayers, starts at 154 K and increases in temperature with coverage.<sup>23</sup> When the multilayer is thick enough the shape of the multilayer desorption peak becomes complicated by the crystallization of ASW to crystalline

ice (CI). This phase change occurs during the temperature ramp, which results in a deflection in the TPD peak.<sup>24,25</sup> For 25 bilayers of ASW deposited on Pt(111) at 22 K, the crystallization occurs at  $\sim 158$  K.<sup>21,24</sup>

Only a few studies have been performed on the interaction between H<sub>2</sub>O and stepped platinum surfaces.<sup>26–29</sup> STM studies on an imperfect Pt(111) crystal show that water adsorbs preferentially on step sites, forming molecular chains.<sup>28</sup> TPD shows a stabilization of the water monolayer by the presence of step sites.<sup>26,27</sup> A two peak structure is observed for a monolayer of H<sub>2</sub>O desorbing from the stepped Pt(533) surface (Pt[4(111)  $\times$  (100)]). At coverages below 0.13 ML a single peak is observed, which Grecea *et al.* reported to shift with coverage from 194 K to 198 K.<sup>27</sup> This peak is associated with desorption from step sites. At higher coverage (above  $\sim 0.33$  ML) a shoulder appears at 185 K, which is associated with desorption from terrace sites. The peak associated with desorption from the water multilayer appears at  $\sim 160$  K.<sup>27</sup>

### 1.6.2 Oxygen on platinum

Oxygen adsorbs in three different states on Pt(111): physisorbed O<sub>2</sub> molecules are stable below 45 K,<sup>30</sup> chemisorbed O<sub>2</sub> molecules below 100 – 200 K,<sup>11</sup> and atomic oxygen below 575 – 900 K.<sup>11</sup> Subsurface oxygen is reported between 1000 and 1200 K if the sample is annealed between these temperatures at high oxygen pressures.<sup>11</sup> Oxygen dissociation is activated and atomic oxygen formation occurs via a precursor state of molecularly adsorbed oxygen. This precursor mechanism causes the sticking coefficient to decrease with surface temperature.<sup>10,31</sup> The maximum O<sub>ad</sub> coverage that can be reached via background dosing is 0.25 ML. LEED<sup>11,32–36</sup> and STM<sup>37</sup> pictures show a (2  $\times$  2) pattern. Oxygen atoms bind preferentially in the fcc hollow sites.<sup>38,39</sup> Higher coverage states can be reached by extended temperature cycling,<sup>40,41</sup> O-beam irradiation,<sup>40</sup> or exposure to NO<sub>2</sub>.<sup>33</sup> Work function change<sup>33,42</sup> and Auger measurements<sup>33</sup> show that the O<sub>ad</sub> in these higher coverage states is chemically similar to low coverage O<sub>ad</sub>. Multiple peaks are seen in TPD spectra, which are probably due to changes in the activation energy of desorption at different coverages.<sup>33</sup> STM images show a p(2  $\times$  1) overlayer structure between 0.25 and 0.50 ML and Pt oxide chains between 0.50 and 0.75 ML.<sup>43</sup>

On stepped surfaces a similar (2  $\times$  2) LEED-pattern is observed for O<sub>ad</sub> as on Pt(111).<sup>9,40</sup> However, Fiorin *et al.* state that no ordered structure of O<sub>ad</sub> atoms is formed on Pt(211) and Pt(411).<sup>44</sup> Dissociation takes place at 200 K<sup>45</sup> on the (111) terrace, but occurs predominantly on step sites<sup>10,46–48</sup> between 150 and 230 K.<sup>44,45,49</sup> Oxygen atoms adsorb preferentially on step sites.<sup>37,48</sup> A combined STM and DFT study<sup>37</sup> shows that for (100) steps a twofold edge bridging site is favored, whereas for (110) steps the fcc hollow site behind the step edge is favored. O<sub>ad</sub> atoms bind stronger on (100) steps than on (110) steps.<sup>44</sup> TPD spectra on Pt(533),<sup>10,45,46,50</sup> other surfaces with (100) steps,<sup>49,51,52</sup> and surfaces with (110) steps<sup>9,32,40,53</sup> all show a

three peak structure in the molecular oxygen regime and a two peak structure in the atomic oxygen regime. Equilibration between step and terrace sites happens only above 400 K.<sup>46</sup> Oxygen atoms do not diffuse onto the lower lying terrace.<sup>48</sup>

On the kinked Pt(321) surface some dissociation of O<sub>2</sub> is already observed at 100 K. The maximum coverage which can be obtained on this surface via background dosing is 3 times larger than on Pt(111).<sup>54</sup>

### 1.6.3 Hydrogen on platinum

Molecular hydrogen adsorbs dissociatively on both Pt(111)<sup>55-57</sup> and stepped platinum surfaces.<sup>58-64</sup> Electron energy loss spectroscopy (EELS) studies in combination with density functional theory (DFT) calculations have shown that on Pt(111) H<sub>ad</sub> binds preferentially in the threefold hollow sites at all coverages.<sup>56,57,65</sup> However, the vibrational modes observed for  $\theta \leq 0.75$  (31 and 68 meV)<sup>56</sup> are different from the ones observed at higher coverages (68, 113, and 153 meV).<sup>57</sup> The modes at low coverages are non-localized, whereas the modes at 68 and 113 meV for  $\theta > 0.75$  can be ascribed to the asymmetric and symmetric stretch at the fcc site modified by anharmonic effects.

The (100) and (110) surfaces show a more complex TPD spectrum than Pt(111). H<sub>ad</sub> binds more strongly to the Pt(100) surface than to the Pt(110) surface.<sup>66</sup> However, reactive force field calculations and experiments show that (110) steps are more reactive towards hydrogen dissociation than (100) steps.<sup>60,67,68</sup> Three different binding sites have been proposed for an H-atom on surfaces with (110) steps. Two of these binding sites are associated with the steps, the other one is associated with the (111) terrace.<sup>59</sup> DFT calculations on Pt(211) (Pt[3(111) × (100)]) show a rather deep global minimum for hydrogen adsorption located at the bridge site on top of the step edge. A high barrier hinders motion from the lower terrace to the step edge.<sup>69</sup> DFT calculations show that the bridge site on the outer atoms is the most stable binding site for a hydrogen atom on (110) sites as well.<sup>70,71</sup>

Quasielastic helium atom scattering (QHAS) measurements on H and D diffusion on Pt(111) indicate that hydrogen diffusion takes place via an isotropic single jump mechanism. A slightly higher barrier for diffusion is found for D<sub>ad</sub> compared to H<sub>ad</sub>.<sup>72</sup> An experimental study on the influence of steps on the diffusion of hydrogen atoms on Pt(111) shows that, compared to the flat Pt(111) surface, both diffusion parallel and diffusion perpendicular to the steps is enhanced by the presence of step sites. For low step densities (miscut angle of 1 or 2° along the  $[\bar{1}1\bar{2}]$  or  $[11\bar{2}]$  direction) diffusion perpendicular to the steps is faster than parallel to the steps. However, for high step densities (miscut angle of 4° along  $[\bar{1}1\bar{2}]$  direction) diffusion perpendicular to the step edges becomes inhibited and slower than on the flat surface.<sup>73</sup>

Recent TPD experiments of hydrogen desorbing from Pt(533) show two desorption features: a large feature below 360 K and a smaller feature at 380 K.<sup>63</sup> The high

temperature feature is associated with recombinative desorption from step sites, whereas the lower temperature desorption feature is associated with recombinative desorption from terrace sites and possibly some remaining step sites. This indicates preferential adsorption of hydrogen on step sites. The entire surface is saturated at  $0.9 \pm 0.05$  ML, whereas the high temperature feature saturates at  $0.14 \pm 0.02$  ML, indicating that only half of the (100) step sites would be covered with  $H_{ad}$ .<sup>63</sup> However, recent experiments from our laboratory report a higher coverage on the step sites of the Pt(533) surface and indicate a non-linear dependence between the ratio  $H_{step} : H_{terrace}$  and step density.<sup>74</sup> The calculations of Olsen *et al.*<sup>69</sup> find that filling the other half of the step sites with hydrogen is energetically more favorable than hydrogen adsorption on terrace sites, though it is 0.05 eV less favorable compared to the first half coverage of  $H_{ad}$  on step sites.

### 1.6.4 Co-adsorption of $H_2O$ and $O_{ad}$ on platinum

The co-adsorption of  $H_2O$  and  $O_2$  on Pt(111) is known to produce  $OH_{ad}$  for  $150 \leq T \leq 185$  K.<sup>16,75,76</sup> When  $^{18}O_2$  and  $H_2^{16}O$  are co-adsorbed at submonolayer coverages and subsequently annealed, the ratio  $^{18}O : ^{16}O$  desorbing in  $H_2O$  is 1 : 2, independent of the initial  $H_2^{16}O$  coverage. Surface OH groups do not readily exchange H with unreacted  $O_{ad}$ .<sup>77</sup> From this stoichiometry initially



was deduced as the reaction equation.<sup>77,78</sup> However, recent DFT calculations found that this reaction does not go to completion and the  $H_{ad}$  is actually incorporated in a hydrogen bonded network of  $H_2O_{ad}$  and  $OH_{ad}$ <sup>15,79</sup> via



All  $O_{ad}$  participates in the OH formation.<sup>16</sup> This produces a  $(\sqrt{3} \times \sqrt{3})R30^\circ$  LEED pattern with a weak  $(3 \times 3)$  superstructure.<sup>14,76,78</sup>  $H_2O$  is needed to stabilize the formed OH species.<sup>16,80</sup> Different structures can be produced by different  $O_{ad} : H_2O$  ratios. The maximum number of  $H_2O$  molecules that can participate in the reaction with one O adatom is four. However, the stoichiometry in equation (1.4) produces the most stable structure.<sup>14</sup>

The hydrogen bonded network consists of hexagonal rings of coplanar O atoms bonded near atop sites with different O—O separations. All H-groups participate in the hydrogen bonded network and OH is always bonded to the platinum substrate via the oxygen atom. All hydrogen bonds lie parallel to the surface.<sup>76,81</sup> One third of the shared protons is delocalized between two O atoms, making them neither clearly covalently bound nor hydrogen bonded to the oxygen atoms.<sup>82</sup> The OH/ $H_2O$  overlayer does not have H-bonds left to bind to a second layer, which makes the surface hydrophobic.<sup>83</sup> When  $H_2O$  is removed, the OH decomposes

again into  $\text{H}_2\text{O}$  and  $\text{O}_{\text{ad}}$ . Water desorption from the O covered surface does not follow simple kinetics and happens through multiple channels: direct desorption, via OH recombination, as well as through proton transfer mediated transportation of water to the edges of an OH/ $\text{H}_2\text{O}$  cluster.<sup>84</sup> Desorption happens primarily at low coordination and defect sites in the OH/ $\text{H}_2\text{O}$  overlayer. HREELS studies on Pt(111) show three separate  $\delta(\text{OH}_{\text{ad}})$  peaks at 127, 113, and 102 meV, associated with structurally different OH-groups. The two lower energy peaks are due to OH-groups which are hydrogen bond donors, but not acceptors.<sup>78</sup> The formed  $\text{OH}_{\text{ad}}$  is also the intermediate in the water formation reaction (WFR). In the presence of gas-phase  $\text{H}_2$  it reacts readily to form  $\text{H}_2\text{O}$ .<sup>85</sup>

$\text{H}_2\text{O}$  adsorbs intact on the reconstructed Pt(110)-(1 × 2) surface.<sup>86</sup> Interestingly, on this surface  $\text{OH}_{\text{ad}}$  formed via the co-adsorption of O and  $\text{H}_2\text{O}$  is not incorporated in a hydrogen bonded network and  $\text{OH}_{\text{ad}}$  remains stable after water desorption up to  $\sim 205$  K.<sup>87</sup>

### 1.6.5 Co-adsorption of $\text{H}_2\text{O}$ and $\text{H}_{\text{ad}}$ on platinum

Flash temperature desorption studies on  $\text{H}_2\text{O}$  desorbing from a hydrogen covered Pt(111) surface<sup>22,88,89</sup> generally show an increase in desorption temperature of the monolayer desorption peak. Different magnitudes for this shift have been reported, ranging from 2 K to 10 K. The monolayer desorption peak saturates at lower coverage than on the bare surface, forcing  $\text{H}_2\text{O}$  molecules into the multilayer desorption peak. A more recent  $\text{D}_2\text{O}$  TPD study<sup>90</sup> involving  $\text{D}_{\text{ad}}$  and  $\text{D}_2\text{O}$  co-adsorption shows that a new peak develops at higher desorption temperatures at the expense of the  $\text{D}_2\text{O}$  desorption feature at 170 K. The desorption temperature of this feature goes through a maximum at 176 K as a function of  $\text{D}_2$  pre-dose. However, at all deuterium pre-coverages the new feature appears at higher temperatures than for the bare surface. Interestingly, on Pt(100) the desorption temperature decreases on the hydrogen covered surface compared to the bare surface.<sup>91</sup>

Isotope labeling studies show exchange between  $\text{D}_{\text{ad}}$  and  $\text{H}_2\text{O}$  co-adsorbed on Pt(111)<sup>89</sup> and Pt(100).<sup>91</sup> HREELS<sup>88,89</sup> and RAIRS<sup>92</sup> studies on the co-adsorption of  $\text{H}_{\text{ad}}$  and  $\text{H}_2\text{O}$  show an additional vibrational feature at  $1150\text{ cm}^{-1}$  at hydrogen coverages above  $\sim 15\%$  after annealing above 150 K. The same feature has been observed on Pt(100).<sup>91</sup> Initially the HREELS data reported no isotopic shift in the  $1150\text{ cm}^{-1}$  peak when  $\text{H}_{\text{ad}}$  was replaced with  $\text{D}_{\text{ad}}$  on Pt(111).<sup>89</sup> Later a disappearance of the peak was reported on Pt(110) when  $\text{D}_{\text{ad}}$  was used.<sup>93</sup> RAIRS studies reported an isotopic shift to  $850\text{ cm}^{-1}$  when  $\text{D}_2\text{O}$  and  $\text{D}_{\text{ad}}$  were co-adsorbed on Pt(111).<sup>92</sup>

The nature of this vibrational feature, and consequently the adsorbed species, has remained elusive. Since the peak is similar to the umbrella mode of  $\text{H}_3\text{O}^+$  in mineral acids, initially it was concluded that a hydronium species was formed, though it was remarked that this did not necessarily imply the transfer of a full

electron.<sup>89</sup> Later Chen *et al.*<sup>93</sup> calculated gas phase vibrational spectra of different water-hydronium complexes and compared them to HREELS spectra on  $(2 \times 1)\text{Pt}(110)$ . They found that the formation of  $\text{H}_3\text{O}^+$  was endothermic and a  $[(\text{H}_2\text{O})_x\text{H}^+]$  complex was a more likely candidate, though the agreement between theory and experiment was not as good as the authors expected. Other species considered were the  $\text{H}_3\text{O}$  radical, a  $\text{H-OH}_2$  complex and anionic complexes. Interestingly the  $1150\text{ cm}^{-1}$  peak is also observed when  $\text{H}_2$  and  $\text{H}_2\text{O}$  are co-adsorbed on the  $\text{Cu}(110)$  surface.<sup>89</sup> However, on  $\text{Cu}(110)$  no isotopic exchange is seen in the desorption spectra and the formation of an hydronium species was excluded on this surface.

On  $\text{Pt}(111)$  Lackey *et al.*<sup>89</sup> have observed an initial decrease of  $\sim 650\text{ mV}$  in the work function when both  $\text{H}_2\text{O}$  and  $\text{H}_2$  are adsorbed. Upon annealing to the temperature where the  $\text{H}/\text{H}_2\text{O}$  species is formed an additional decrease of  $\sim 100\text{ mV}$  in the work function is reported. It was concluded that the formed species is positively charged, even though the decrease in the work function is not as large as expected for the transfer of a full electron. The change in work function could also be caused by a dipole rearrangement in water ice.<sup>94</sup>

### 1.6.6 Electrochemistry

The electrochemical signature of the platinum–aqueous electrolyte interface is its blank cyclic voltammetry (CV). On  $\text{Pt}(111)$  the peak observed between 0.6 and 0.9 V versus the reversible hydrogen electrode (RHE) is considered to be due to the adsorption of OH from dissociated  $\text{H}_2\text{O}$  on terrace sites. At higher potentials  $\text{OH}_{\text{ad}}$  is converted into  $\text{O}_{\text{ad}}$ . The same oxygen containing species are observed on polycrystalline platinum surfaces. However, the formation of  $\text{OH}_{\text{ad}}$  and  $\text{O}_{\text{ad}}$  occurs simultaneously at these surfaces.<sup>95</sup> On regularly stepped platinum surfaces only  $\text{OH}_{\text{ad}}$  formation on terrace sites has been identified (at a similar potential region as  $\text{OH}_{\text{ad}}$  formation on  $\text{Pt}(111)$ ).<sup>96</sup> So far, no  $\text{OH}_{\text{ad}}$  formation on step sites has been identified.

The underpotential deposition of hydrogen ( $\text{H}_{\text{upd}}$ ) on  $\text{Pt}(111)$  occurs between 0.05 and  $0.35\text{ V}_{\text{RHE}}$ . The evolution of  $\text{H}_2$  takes place through the formation of overpotential deposited hydrogen at lower potentials ( $\text{H}_{\text{opd}}$ ).<sup>96</sup> In alkaline media the kinetics of hydrogen adsorption are significantly slower than in acidic media.<sup>97,98</sup> The adsorption of hydrogen at the  $\text{Pt}(111)$ /electrolyte interface is well approximated by a mean-field (or "Frumkin") isotherm, implying relatively weak repulsive interactions between the adsorbed UPD hydrogen.<sup>99–101</sup> Upon the introduction of step sites on the surface an additional sharp peak is observed in the  $\text{H}_{\text{upd}}$  region. Traditionally, this feature is ascribed to the adsorption-desorption of hydrogen at the step. The shape of the feature implies attractive interactions between adsorbed hydrogens at step sites.<sup>102</sup> This is in stark contrast to the repulsive interactions observed at terrace sites.